A multi-faceted, environmental forensic characterization of a paradigmatic brownfield polluted by hazardous waste containing Hg, As, PAHs and dioxins

Begoña Fernández[1], Luis M. Lara[2], Juan M. Menéndez-Aguado[2], Julia Ayala[1], Nerea García-González[2], Lorena Salgado[2], Arturo Colina[2], José Luis R. Gallego[2*]

Environmental Technology, Biotechnology and Geochemistry Group. Laboratorio de Metalurgia. Escuela de Minas Energía y Materiales. Universidad de Oviedo. Independencia 13, 33004, Oviedo, Spain

Environmental Technology, Biotechnology and Geochemistry Group. INDUROT. Campus de Mieres, University of Oviedo, C/Gonzalo Gutiérrez Quirós. S/N, 33600 Mieres, Spain

(*) Corresponding author

Abstract

Hg and As mining-metallurgy plants have severely impacted environmental compartments. In this context, La Soterraña site (northern Spain) is a paradigmatic site that has been studied in terms of soil, water and vegetation pollution. However, here we used a novel multi-purpose forensic approach to determine the characteristics of the main source of pollution that is still active at the site, namely the waste deposits that built up over decades. This approach included advanced analytics focused not only on the main mining-metallurgical waste but also construction and demolition (C&D) waste as a potential repository of hazardous pollutants. In addition, we used GC-MS techniques to perform a detailed assessment of organic pollution. Our results indicate that most of the C&D waste should be considered hazardous, although, as expected, waste from the metallurgy industry raises maximum concern. The presence of extremely high concentrations of Hg and As in very fine grain-size fractions of the waste, the extent of As mobility found, and the co-occurrence of organic contaminants (PAHs, dioxins, etc.) and unexpected toxic organometallics confirm that La Soterraña is one of the most polluted sites in Europe. This scenario therefore calls for an urgent clean-up campaign.

Keywords

Hazardous waste; Arsenic; Mercury; PAHs; Dioxins.

*Graphical Abstract

A multi-faceted, environmental forensic characterization of a paradigmatic brownfield polluted by hazardous waste containing Hg, As, PAHs and dioxins

(Fernández et al., 2020)

Graphical abstract

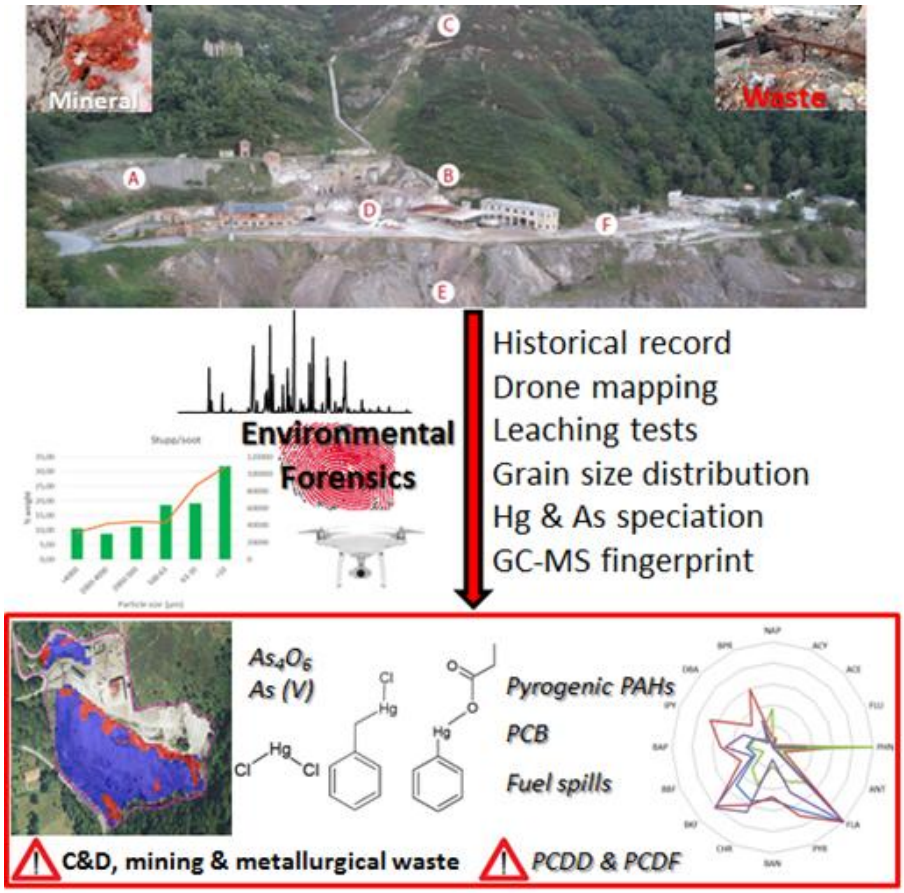

A multi-faceted, environmental forensic characterization of a paradigmatic brownfield polluted by hazardous waste containing Hg, As, PAHs and dioxins

(Fernández et al., 2020)

Highlights

A multifaceted forensic approach revealed severe pollution in a brownfield.

C&D waste contains As and Hg.

Complex speciation, including unforeseen Hg-aromatic compounds, examined.

PAH ratios and distribution revealed pyrogenic sources.

Hg-pyrometallurgy processes produced dioxins and furans.

A multi-faceted, environmental forensic characterization of a paradigmatic brownfield polluted by hazardous waste containing Hg, As, PAHs and dioxins

Begoña Fernández[1], Luis M. Lara[2], Juan M. Menéndez-Aguado[2], Julia Ayala[1], Nerea García-González[2], Lorena Salgado[2], Arturo Colina[2], José Luis R. Gallego[2*]

Environmental Technology, Biotechnology and Geochemistry Group. Laboratorio de Metalurgia. Escuela de Minas Energía y Materiales. Universidad de Oviedo. Independencia 13, 33004, Oviedo, Spain

Environmental Technology, Biotechnology and Geochemistry Group. INDUROT. Campus de Mieres, University of Oviedo, C/Gonzalo Gutiérrez Quirós. S/N, 33600 Mieres, Spain

(*) Corresponding author

Abstract

Hg and As mining-metallurgy plants have severely impacted environmental compartments. In this context, La Soterraña site (northern Spain) is a paradigmatic site that has been studied in terms of soil, water and vegetation pollution. However, here we used a novel multi-purpose forensic approach to determine the characteristics of the main source of pollution that is still active at the site, namely the waste deposits that built up over decades. This approach included advanced analytics focused not only on the main mining-metallurgical waste but also construction and demolition (C&D) waste as a potential repository of hazardous pollutants. In addition, we used GC-MS techniques to perform a detailed assessment of organic pollution. Our results indicate that most of the C&D waste should be considered hazardous, although, as expected, waste from the metallurgy industry raises maximum concern. The presence of extremely high concentrations of Hg and As in very fine grain-size fractions of the waste, the extent of As mobility found, and the co-occurrence of organic contaminants (PAHs, dioxins, etc.) and unexpected toxic organometallics confirm that La Soterraña is one of the most polluted sites in Europe. This scenario therefore calls for an urgent clean-up campaign.

Keywords

Hazardous waste; Arsenic; Mercury; PAHs; Dioxins.

1. Introduction

Former industrial and mining sites (brownfields) are usually affected by mixtures of pollutants that have been released into the environment or have been disposed of inappropriately. The co-occurrence of such complex mixtures poses a challenge for site remediation. In this context, a forensic approach (Alker et al., 2000; Gallego et al., 2016; Hagmann et al., 2019), including advanced analytical methods, is often required to identify the distinctive features of source-specific contamination (Morrison and Murphy, 2006; Uhler et al., 2010). Balancing the attributes of different target and non-target analytical methods is therefore advantageous for the comprehensive chemical fingerprinting of these sites (Lara-Gonzalo et al., 2015).

With respect to the environmental risks associated with brownfields, the mobilization of potentially toxic elements (PTE) in abandoned mining areas has been widely studied (Ahn et al., 2005; Álvarez-Ayuso et al., 2012; Bindler et al., 2012; Chopin and Alloway, 2007; Gray et al., 2002; Moore and Luoma, 1990; Riewerts et al., 2014). Hg, for instance, is the focus of the Minamata convention and has received considerable attention (Evers et al., 2016; Liu et al., 2012; UNEP, 2013). This metal has a complex biogeochemical cycle, and ionic Hg can be converted into alkyl-Hg compounds, which are highly toxic (He et al., 2019). In turn, it is widely recognized that As poses a threat to public health (Haffert and Craw, 2008; Tarvainen et al., 2013). Arsenic toxicity causes environmental problems worldwide, in particular in relation to natural groundwater (Wang et al., 2018; Wilkin et al., 2018). Indeed, mine tailings and their effluents usually contain high concentrations of As and are thus one of the main anthropogenic sources of this contaminant (Wang and Mulligan, 2006).

Until the 1970s, the Asturian mining region in northern Spain was one of the largest Hg-producing regions in the world. Most of the ores exploited contained both As and Hg (Loredo et al, 1988). The environmental effects of such mining activity have been extensively addressed in recent decades (Higueras et al., 2015; Loredo et al., 1999), together with approaches for the treatment of polluted soils and waters (Boente et al, 2018; Fernández et al., 2017; Gil-Díaz et al., 2019; Sierra et al., 2013). Of the former Hg-sites in the region, two processing plants were particularly relevant because of the concurrence of mining activity and metallurgical processes. The former metallurgical activity of the first plant, known as El Terronal, and its dramatic effects on the environmental compartments has been widely studied (Gallego et al., 2015; González-

Fernández et al., 2018). The second plant, known as La Soterraña, presents similar problems (Loredo et al., 2006) and has been evaluated from various perspectives with the aim to propose potential remediation measures (Ayala and Fernández, 2019; Matanzas et al. 2017; Sierra et al., 2011). However, a detailed forensic study of the main sources of pollution (different types of waste) and their leachability has not been done to date. Furthermore, the abandoned buildings and installations have not been fully described, nor have combined studies taken into consideration the potential presence of organic contaminants.

To properly manage environmental hazards in brownfields, analyses should address not only stock-piles of distinct industrial or mining waste but also construction & demolition (C&D) waste (Somasundaram et al., 2015; Staunton et al., 2014). Therefore, in sites with a severe metal and metalloid pollutant load, C&D waste should be taken into account (Saca et al., 2017). In turn, Hg-sites are commonly characterized by the co-occurrence of organic contaminants (Gallego et al., 2015). This feature deserves further attention given that brownfields commonly house installations related to organic pollution, such as underground storage tanks, transformers, and high-temperature ovens (Lara-Gonzalo et al., 2015). C&D waste can also include organic pollutants (Butera et al., 2014; Jang and Towsend, 2001). In this regard, it should be noted that the methodical evaluation of the co-occurrence of organic and heavy metal(loid)s in brownfield sites is uncommon (Gallego et al., 2016; Thavamani et al., 2011). Notably, gas chromatography-mass spectrometry (GC-MS) techniques have proved powerful tools for environmental studies and for the chemical fingerprinting of organic compounds, especially in the case of complex mixtures and processes such as weathering (Douglas et al., 2007; Kruge et al., 2018; Uhler et al., 2010).

In the context of organic and PTE pollution in brownfield sites, here we conducted a multifaceted, environmental, forensic evaluation of La Soterraña, including the consideration of C&D waste and a detailed analysis of potential organic contaminants (PAHs, PCBs, dioxins and others). This integral and exemplifying study: i) provides a comprehensive classification of the waste found, including volumes and surfaces affected; ii) addresses the mechanisms of pollutant dispersal in the surroundings of the brownfield; iii) identifies sources of organic pollutants on the site; and iv) sets out a comprehensive approach to evaluate the study site, including toxicological features and potential remediation measures.

2. Materials and methods

2.1 Historical data, site description and samples

The site of La Soterraña (Fig. 1A) is located in Asturias (NW Spain). It was used for decades—until its closure in 1974—for the exploitation of an underground Hg mine and for the metallurgical processing of Hg ores from that mine and others in the vicinity. The main characteristics of the site (ore geology, geomorphology, vegetation, weather, etc.) have been described previously (see Matanzas et al., 2017 and references therein). As a general overview (see results for details), the site currently consists of a wide platform where the main installations and ruins of buildings are located. The first soil-heap and the old chimneys are located uphill of this area, while a larger spoil heap is located downhill (Fig. 1B).

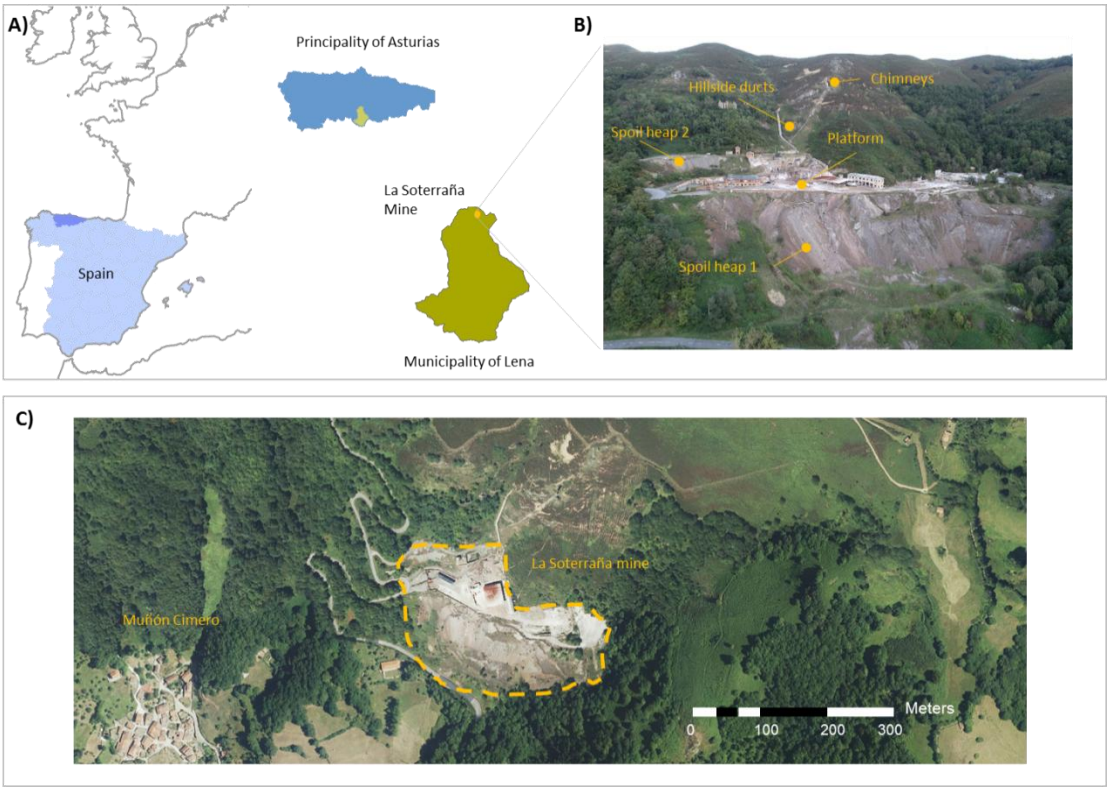

Figure 1: A) Location of the study site in NW Spain (43º11'34" N, 5º50'36" W). B) Current front-view of La Soterraña site and the main installations. C) Aerial view of La Soterraña and distance (below 500 m) to the closest populated areas.

We studied the historical information available, including aerial views from different dates, an initial detailed in situ reconnaissance, and a detailed cartography of the site (drone flight carried out with a Phantom IV Pro at 70 m altitude and the subsequent GIS processing), thereby identifying the buildings on the main platform of the pyrometallurgy plant, the surrounding spoil heaps, and the duct/chimney area. The volumes and surfaces of the aforementioned elements within the site were estimated by the "volume calculations tools" of Arcmap 10.3 on the digital surface model previously obtained from high-resolution drone imagery (processed with Pix4Dmapper 4.3.31 photogrammetry software).

Subsequently, we designed and performed a scrupulous sampling of 27 distinct waste materials (see Fig 2. in Results for specific location of the samples). Composite samples (ranging from 200 g to several kg depending on their typology) were collected and stored in plastic bags. The sampled materials were brushed lightly in situ to remove recent dust. When needed, a clean stainless steel tool was used to scrape fragments and fine material off the first centimetres of the C&D waste found (wall coverings, brick surfaces, etc.).

2.2 Elemental analysis

Composite samples were initially screened and sorted (different types of waste) by means of semi quantitative x-ray fluorescence using dispersed energy (FRX-ED) in a Shimadzu spectrometer (EDX-720HS) equipped with a Si(Li) detector.

After the initial classification, representative waste subsamples were dried at room temperature in order to minimize the loss of volatile contaminants. They were then disaggregated by a roller in order to facilitate sieving through a 4-mm screen. Materials with a grain-size greater than 4 mm were vigorously washed and rubbed to recover fine particles adhered to the gravels and pebbles, which, once cleaned, were excluded from the study. The final material was mechanically split (riffle) to obtain 50-g representative subsamples and then pulverized to a particle size of less than 100 μm. All utensils were thoroughly cleaned with ethanol between samples. For multi-element analysis, 0.250-g representative subsamples were leached by means of an 'Aqua regia' digestion ($HCl+HNO_3$) in an Anton Paar 3000 microwave. The samples were diluted and filtered.

As and Hg were quantified by an Inductively Coupled Plasma Mass Spectrometer (ICP-MS 7700, Agilent Technologies) using IDA (Isotope Dilution Analysis).

2.3 Leaching tests

Compliance testing was conducted to check whether the samples satisfied widely accepted waste regulations. To this end, the waste materials were classified using the UNE-EN 12457-3:2004 test and USEPA Method 1311 (TCLP, Toxicity Characteristic Leaching Procedure).

The UNE-EN 12457-3:2004 test was applied with a liquid/solid (L/S) ratio of 10 l/kg, and deionized water as a leaching liquid. This method involved stirring the solution for 24 h and then leaving the samples to decant. The solution was then passed through a membrane filter (0.45 μm), and a subsample of the leachate was taken for each material for further analysis by ICP-MS.

The TCLP test was performed to evaluate the potential mobility and availability of As and Hg in the waste samples. An acetic acid-based TCLP extraction fluid was prepared with 2.572 g of NaOH and 5.72 mL of glacial acetic acid (pH 4.93 ± 0.05). This test involved stirring 1 g of sample with 20 ml of leaching liquid. After 18 h of mixing, the leachate was passed through a Millipore 0.4-μm filter. The pH of the filtrate was then measured, and the leachate was acidified with a small amount of nitric acid to a pH less than 2, followed by ICP-MS analysis.

2.4 Chemical speciation

As and Hg species were measured in order to obtain more information about the potential toxicity of the wastes. In brief, to measure the former, 0.1 g of waste and an extracting agent (1 M H_3PO_4+ 0.1 M ascorbic acid) were placed in a microwave vessel. The extracts were diluted and filtered. The As species were split with a mobile phase of 2 M PBS (Phosphate Buffered Saline)/0.2 M EDTA (pH = 6.0) in a separation column with a 1260 Infinity HPLC coupled to the ICP-MS described above. In addition, Hg species were extracted using a solution of 7.6% HCl and 10% 2-mercaptoethanol in an ultrasonic bath. The extract was then centrifuged and diluted. The determination was carried out in a HPLC apparatus coupled to ICP-MS, using a ZORBAX Eclipse XDB C18 (2.1 mm i.d. × 50 mm, 5 μm) column and 0.06 M ammonium acetate, 5% methanol and 0.1% 2-mercaptoethanol (pH = 6.8) as mobile phase.

2.5 *Grain-size distribution*

Particle size distribution tests were performed by wet sieving 1 kg of another set of representative subsamples (only for mining and metallurgical waste) to obtain particle-size fractions of <63, 63-500, 500-2000, 2000-4000 and >4000 µm. The grain-size distribution of the <63 µm fraction was obtained in a Beckman Coulter particle sizing analyzer, model LS 13 320, using the Aqueous Liquid Module (ALM) with an auto-sampler. In addition, to obtain sub-samples in the size intervals of 10-63 µm and <10 µm, classification tests were performed in a hydrocyclone Mozley C124 rig (currently provided by Salter Cyclones). The separation conditions used were established after some preliminary tests and consisted of a cyclone diameter of 50.8 mm, underflow diameter of 9.5 mm, overflow diameter of 14.6 mm, 0.2 bar of pressure and a solids feed of 15% wt.

2.6 *Organic analysis*

Aliquots of the same 27 samples used for inorganic analysis were considered for organic pollutant assessment. Also, two additional samples (see section 3.1) were taken, both showing evident organoleptic properties, thereby suggesting hydrocarbon and PCB content, respectively.

GC-MS screening

1-g representative subsamples were extracted with hexane:dichloromethane (1:1, v/v) in a Soxtherm system (Gerhardt). The extract was concentrated by rotary evaporation. Aliquots of the Soxtherm extract were fractionated and gravimetrically quantified by LC (Liquid Chromatography) steps in the case of pure products (the two additional samples described above), whereas the extracts of the other 27 samples were directly injected into the chromatograph after rotary evaporation. For LC, maltenes and asphaltenes were separated by passing the extract through 0.45-µm filters using hexane and dichloromethane, respectively. Maltenes were then split into saturated, aromatic, and polar fractions by LC in columns filled with silica gel and alumina (saturates were eluted with hexane, aromatics with a mix of dichloromethane:hexane (4:1, v/v) and the polar fraction with methanol).

Direct extracts and LC fractions were analyzed by GC/MS (Gas Chromatography – Mass Spectrometry). The extracts were injected into a 7890A GC System coupled to a

5975C Inert XL MSD with Triple-Axis Detector (Agilent Technologies). A capillary column DB-5ms (5% phenyl 95% dimethylpolysiloxane) 30 m × 0.25 mm i.d. × 0.25 μm film (Agilent Technologies) was used, with helium as carrier gas at 1 mL/min. The initial oven temperature was 40ºC (held for 5 min) and was ramped up at 5ºC/min to 300ºC (held for 20 min). The mass spectrometer was operated in electron ionization mode (EI) at 70 eV and was calibrated daily by auto-tuning with perfluorotributylamine (PFTBA). The chromatograms were acquired in full-scan mode (mass range acquisition from 45 to 500 m/z).

PAH and PCB quantification

After Soxhterm extraction (see above) with Dichloromethane:Acetone (1:1), the 16 priority PAHs were quantified in the same GC/MS described above. In this case, the initial oven temperature was 70ºC (held for 2 min) and was ramped up at 20ºC/min to 220ºC, raised to 270ºC at 10ºC/min (held for 1 min), then raised to 290ºC at 10ºC/min (held for 1 min), and finally ramped up at 10ºC/min to 300ºC (held for 7 min). The GC injector was operated in splitless mode for 2 min, and its temperature was maintained at 260ºC. The mass spectrometer was operated in selected ion monitoring mode (SIM), and the quantification of m/z relations was as follows: 128 (Naphthalene); 152, 153 and 154 (Acenaphthylene and Acenaphthene); 165 and 166 (Fluorene); 178 (Phenanthrene and Anthracene); 202 (Fluoranthene and Pyrene); 228 (Benz[a]anthracene and Chrysene); 252 (Benzo[b]fluoranthene, Benzo[k]fluoranthene and Benzo[a]pyrene); and 276 and 278 (Dibenz[a,h]anthracene, Benzo[ghi]perylene and Indene[1,2,3-cd]pyrene). We also measured the PCB Congener Content Evaluation Revised Mix 1 in the same GC/MS device. To do so, the initial oven temperature was 50ºC (held for 1 min) and was ramped up at 30ºC/min to 200ºC (held for 2 min), and finally ramped up to 10ºC/min to 300ºC (held for 15 min). The GC injector was operated in splitless mode, and its temperature was maintained at 280ºC. The mass spectrometer was operated in SIM, and the quantification of m/z relations was as follows: 186, 256, 258 (2,4,4´-Trichlorobiphenyl); 220, 290, 292 (2,2´,5,5´- Tetrachlorobiphenyl); 256, 326, 328 (2,2´,4,5,5´- Pentachlorobiphenyl); 256, 326, 328 (2,3´,4,4´,5- Pentachlorobiphenyl); 290,360,362 (2,2´,3,4,4´,5´- Hexachlorobiphenyl); 290, 360, 362 (2,2´,4,4´,5,5´-Hexachlorobiphenyl); and 324, 394, 396 (2,2´,3,4,4´,5,5´- Heptachlorobiphenyl).

Dioxins and Furans

To quantify tetra- through to octa-chlorinated dioxins and furans (PCDD and PCDF), samples were extracted, cleaned up, fractionated and then analyzed by isotope dilution and HRGC-HRMS following EPA Method 1613 requirements. PCDDs and PCDFs were identified with a Trace GC Ultra coupled to a DFS high resolution magnetic sector mass spectrometer (GC-HRMS) from Thermo Scientific. The capillary column was a TR-DIOXIN-5 ms 60 m × 0.25 mm i.d. × 0.25 μm film (Thermo Scientific). The initial oven temperature was 140ºC (held for 1 min) and was ramped to 200ºC at 20 ºC/min and held for 3 min, then raised to 310ºC at 3 ºC/min and held for 8 min, and finally raised to 325ºC and held for 5 min. The carrier gas was helium at a column flow of 1 mL/min. The HRMS detector was operated in MID (Multiple Ion Detection) mode. The identification and quantification of congeners and the calculation of the toxicity equivalents were done by isotope dilution analysis following EPA Method 1613 and using the software TargetQuan by Thermo Scientific.

3. Results

3.1 Site reconnaissance and selection of samples

This section provides a summary of the background information about the activities undertaken in the plant, and the reconnaissance and cartography data obtained (Fig. 2A). The site has different sub-areas according to the activities that were developed; i.e. mining activity, ore processing and metallurgy, auxiliary processes, etc. After several decades of abandonment, the site is fully derelict and only some of the structures (partial ruins) are still standing. In this context, the main elements of the site can be classified into three main groups (see detailed photographs in Fig. S1, supplementary material): (i) platform zone where the mine and metallurgical activities were carried out, including 20 derelict buildings (only 5 still standing although damaged). C&D and metallurgical waste are distributed unevenly and the remains of the old ovens and condensation systems can be observed; (ii) mine waste spoil heaps covering a total area of 2.9 ha divided in two separate dumps, one in the upper part (northern spoil heap, smaller size, labelled SH2 in Fig. 2B) of the platform and the other in the lower part (southern spoil hear, larger size, labelled SH1 in Fig. 2B); and (iii) the ruins of five hillside ducts (between 150 and 350 m long) running along the southern slope of the hill up to vertical chimneys (up to 13 m high). Note that gases from the furnace were released into the atmosphere through these hillside chimneys of distinct diameters.

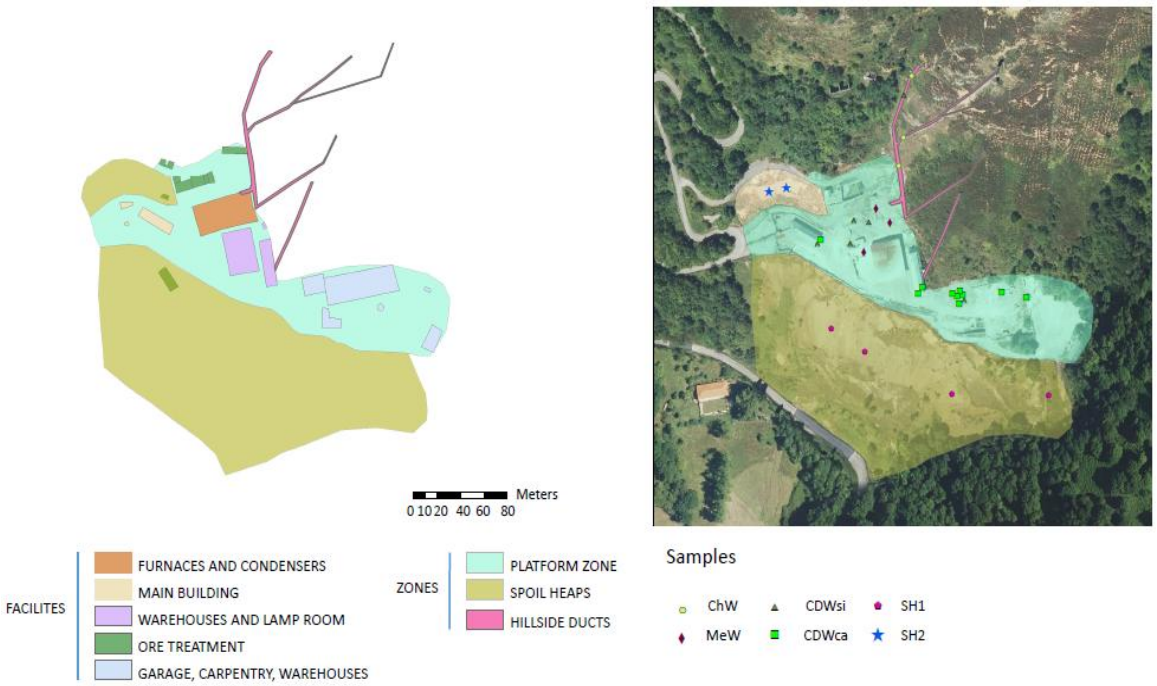

298

299 Figure 2: A) Main facilities and subdivision of the site into zones. B) Sample locations
300 (SH: Spoil heaps; MeW: Metallurgy waste; CDW: Construction & Demolition Waste;
301 ChW: Chimney Waste –Flue Dust-).

302

303 Samples were collected within the areas described above with the following distribution
304 and sorting (Fig. 2B):

305 ✓ Mining waste: Four representative samples were collected in the larger spoil heap
306 (southern, SH1) and two in the smaller one (northern, SH2).
307 ✓ Metallurgical waste: Following the previous description abovementioned (Gallego
308 et al., 2015), 3 representative samples of stupp/soot waste (MeW in Fig. 2B) and 3
309 samples of flue dust (ChW in Fig. 2B) were taken. In brief, stupp/soot is a mixture
310 of As-enriched dust recovered in the first stage of the Hg purification/condensation
311 system, and Hg-rich soot is a dark residue consisting of Hg-soot and Hg-ore dust.
312 On the other hand, flue dust is a mixture of the slurry formed during the cleaning of
313 the chimneys and some As- and Hg-rich soot and dusts that were not retained in the
314 purification/condensation systems.
315 ✓ Construction & demolition waste: Up to 15 different types of debris and wall
316 material were sampled in the remaining buildings and rubble. An initial XRF
317 screening of these samples suggested a division between limestone-gypsum type (9

samples, labelled CDW_{Ca} in Fig. 2B) and ceramic-metallic type (6 samples, labelled CDW_{Si} in Fig. 2B).

- ✓ Organic residues: Spilled fuel oil from the underground storage tanks used in the ovens and a blackish residue found beneath the zone housing the former transformers were also sampled.

3.2 Waste total concentration, leachability, speciation and volumes

Samples classified as mining, metallurgy or C&D waste were studied by ICP-MS measurements of total concentrations and the two types of leachates described above. The main results are summarized in Table 1.

Table 1: Total concentration of As and Hg, leachates and chemical speciation.

Waste type (sample label, see Fig 2B), number of samples		**Average total ± dev. (g/t)**		***Leachates (%)***					
				UNE-EN 12457 (H_2O)		*US-EPA 1311 (TCLP)*		HPLC-MS speciation (%)	
		As	**Hg**	***As***	***Hg***	***As***	***Hg***	**As (III)**	**Methyl-Hg**
Mining waste	**Spoil heap 1 (SH1), n=4**	15,000±2,210	890±170	*0.2*	*<0.1*	*3.2*	*<0.1*	2.1	0
	Spoil heap 2 (SH2), n=2	23,000±250	6,000±1,610	*0.2*	*<0.1*	*0.4*	*<0.1*	0.3	0
C&D Waste	**Limestone-gypsum (CDW_{Ca}), n=9**	2,120±980	30±20	*3.0*	*0.1*	*12.0*	*<0.1*	0	0
	Ceramic-metallic (CDW_{Si}), n=6	64,830±11,600	14,680±10,320	*1.9*	*0.2*	*5.4*	*<0.1*	0	0
Metallurgical waste	**Stupp/soot (MeW), n=3**	95,900±51,620	107,100±24,640	*2.2*	*<0.1*	*12.0*	*<0.1*	15.0	0
	Flue dust (ChW), n=3	138,200±25,800	33,000±6,900	*14.2*	*<0.1*	*14.8*	*<0.1*	64.6	0

In general terms, Hg leachability was very low with both methods used. In contrast, As leachability was significant, not correlated with the total concentrations, and higher using the US-EPA 1311 (TCLP, slightly acidic) than the UNE-EN 12457 method (H_2O, neutral). Metallurgical wastes presented the highest percentages of leachability,

334 although C&D waste limestone-gypsum type also showed high values for As. Finally,
335 mining waste presented lower values in the leachate measurements. On the other hand,
336 analysis of As and Hg speciation (also shown in Table 1) revealed the absence of
337 methyl-Hg (more toxic than inorganic Hg), and a heterogonous abundance of As (III)
338 (more toxic than As (V)), which was particularly abundant in the metallurgical waste.

339 Finally, and in addition to the chemical characterization, we calculated the surficial area
340 and volumes of the different waste using a compilation of the cartographic data reported
341 by the drone flight, other previous aerial views, former studies (Loredo et al., 2006;
342 Luque, 1985, and references therein), and the *in situ* reconnaissance carried out in this
343 work. Our results (Table S1) highlighted the vast amount of waste accumulated in the
344 main spoil heap (around 200,000 t), and a remarkable estimated total mass of Hg
345 (hundreds of tons, particularly in the metallurgical waste) and particularly of As
346 (thousands of tons, particularly in the mining waste) still present in the study site.
347
348
349 *3.3 Grain-size study of mining and metallurgical waste*

350 Only mining and metallurgical wastes (because of their volume and very high
351 contaminant content) were subjected to grain-size studies. Fig. 3 shows the merged
352 results of the wet sieving and laser diffraction grain-size analyses for the representative
353 subsamples examined.

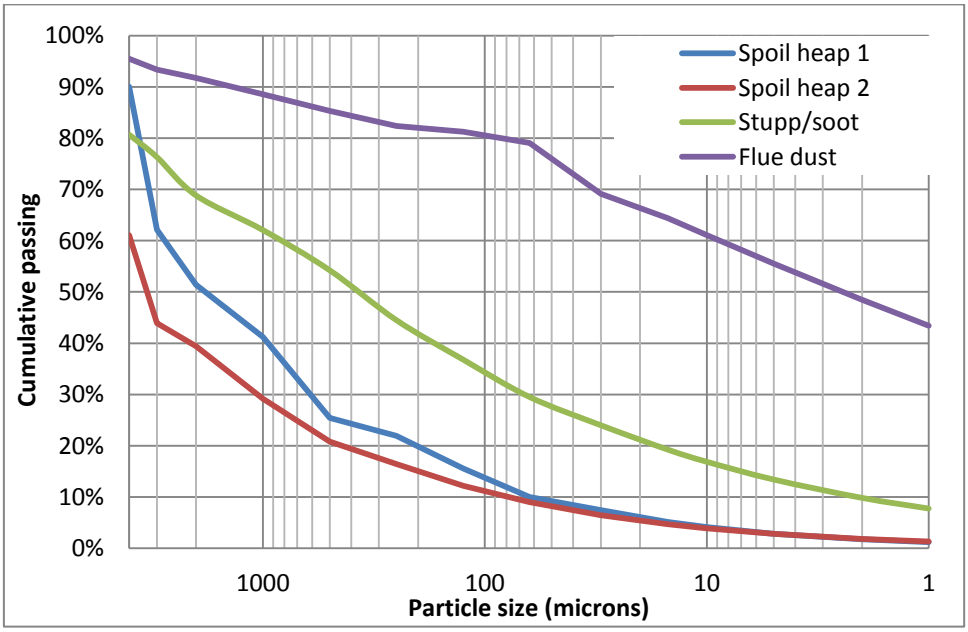

354

Figure 3: Grain-size analyses of mining and metallurgical waste (wet sieving + laser diffraction).

The grain-size curves indicate a distinct distribution of fractions between mining waste in the spoil heaps (thicker, with d_{50} well-above 1 mm) and metallurgical waste (d_{50} notably lower, especially for flue dust, which was below 10 µm).

Regarding the distribution of As and Hg, the grain-size fractions obtained by wet-sieving (63-500, 500-2000, 2000-4000 and >4000 µm) and hydrocycloning (10-63 and <10 µm) were subjected to ICP-MS analysis. The concentrations of Hg and As (lines in the figure) increased as the grain-size decreased, with the exception of Hg in the metallurgical waste. In contrast, when percentages in weight were evaluated (bars in the figure), As and Hg were predominant in the finer fractions of the flue dust while As was also predominant in stupp/soot (Fig. 4).

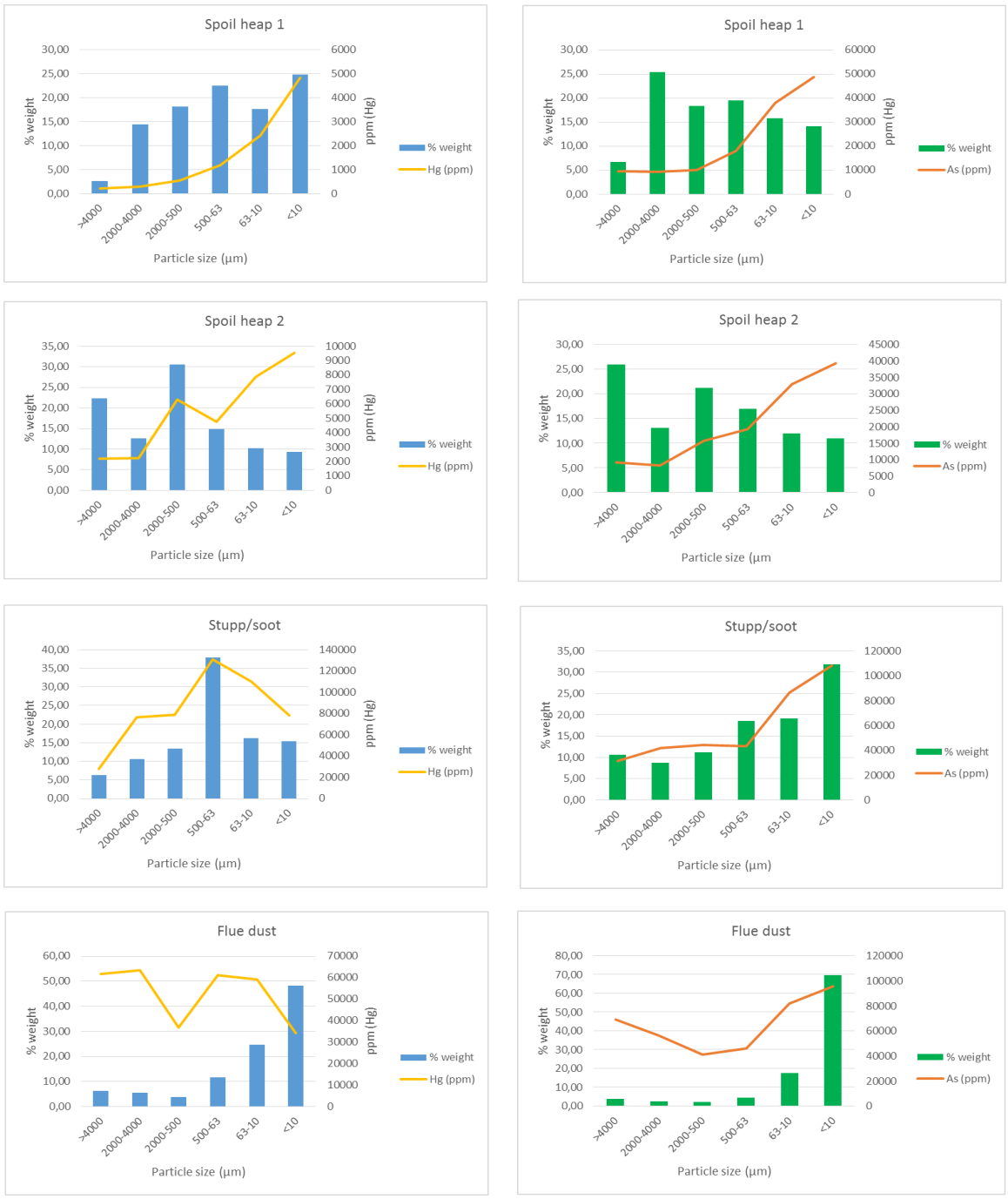

Figure 4: Distribution of Hg (left graphs) and As (right) in the representative subsamples of mining and metallurgical waste subjected to grain-size fractionation by wet sieving, and subsequent ICP-MS determination of elemental contents.

3.4 Organic pollution

3.4.1 Spills

The two "pure" organic residues found in some of the former installations of the site (Section 2.6) were analyzed. The first product was found in the vicinity of the underground storage tanks. LC results revealed a mixture of 30% saturates, 38% aromatics, and significant amounts of non-distillable fractions (15% resins and 17% asphaltenes), thereby strongly suggesting a probable match with heavy fuel oil. In addition, the main features of the fingerprint of the product (Fig. S2A) were a prominent UCM (Unresolved Complex Mixture), a very low abundance of n-alkanes consistent with a depleted C18/Phytane ratio, the abundance of hopanes and of S compounds (mainly dibenzothiophenes), and the absence of light aromatics (Fig. S2B). Taken together, these findings support the notion of a very long weathering process (Kruge et al., 2018) and the usual preferential degradation of n-alkanes compared with isoprenoids or hopanes (Gallego et al., 2007, Hagmann et al., 2019). As regards the other spillage identified in the detailed reconnaissance of the study area, PCB congeners were found in notable amounts (up to more than 1,000 ppm), thereby revealing the classical Aroclor fingerprint (Nikonova and Gorshkov, 2011) (Fig. S2C).

3.4.2 PAH contents in different waste and fingerprinting of organic pollution

Representative aliquots of the 27 waste samples were initially screened by qualitative full-scan GC-MS. The results revealed the presence of PAHs as the predominant group of organic contaminants in most of the samples irrespective of the type of waste, although especially abundant in mining and metallurgical waste. Other compounds identified in some of the chromatograms were PCBs and aliphatic compounds, both families of compounds probably linked to the dispersal of spilled products, such as those described in the previous section. PAH quantification (Table 2) showed very different data as regards the different type of waste; i.e. notable content in metallurgical waste, moderate or low in mining waste, and negligible or below detection limit in C&D debris (not included in Table 2). In all cases, 3-4-ring compounds predominated.

Table 2: PAH content in selected samples: 2-ring PAHs (naphthalene); 3-ring PAHs (fluorene + acenaphthylene + acenaphthene + phenanthrene + anthracene); 4-ring PAHs (fluoranthene + pyrene + benz[*a*]anthracene + chrysene); 5–6 ring PAHs (benzo[*b*]fluoranthene + benzo[*k*]fluoranthene + benzo[*a*]pyrene + dibenz[*a*,*h*]anthracene + benzo[*ghi*]perylene + indeno[1,2,3-*cd*]pyrene).

Waste type		**Samples (n)**	**PAHs (mg/kg)**			
			2-ring	**3-4 rings**	**5-6 rings**	***Total***
Mining waste	**Spoil heap 1**	4	0.05	0.17	0.09	*0.30*
	Spoil heap 2	2	0.20	0.24	0.10	*0.55*
Metallurgical waste	**Soot –Stupp**	3	1.81	6.73	1.43	*9.98*
	Flue dust	3	0.39	3.50	1.19	*5.09*

The distribution of individual PAHs in the four types of metallurgical and mining waste sampled revealed a relatively homogeneous distribution, thereby suggesting a common source (Fig. S3). In addition (see Fig. 5), there was a very low abundance of alkyl-PAHs (typical of crude oil derivatives), and conversely a notable abundance of parent-PAHs, thus pointing to a pyrogenic origin (Kruge et al., 2018).

Finally, a detailed GC-MS fingerprint of the organic extracts of the metallurgical waste is shown in Fig. 5. Together with the previously described presence of PAHs, of note is the abundance of Hg^0, some Hg organometallic compounds, and even Hg (II) chloride (the mass spectra of these Hg compounds is shown in Fig S4). In addition, oxygenated-PAHs (OPAHs) were also present and prominent. Several PCB congeners, and sulphur heterocycles were also identified, but in relative concentrations that were too low to produce visible peaks.

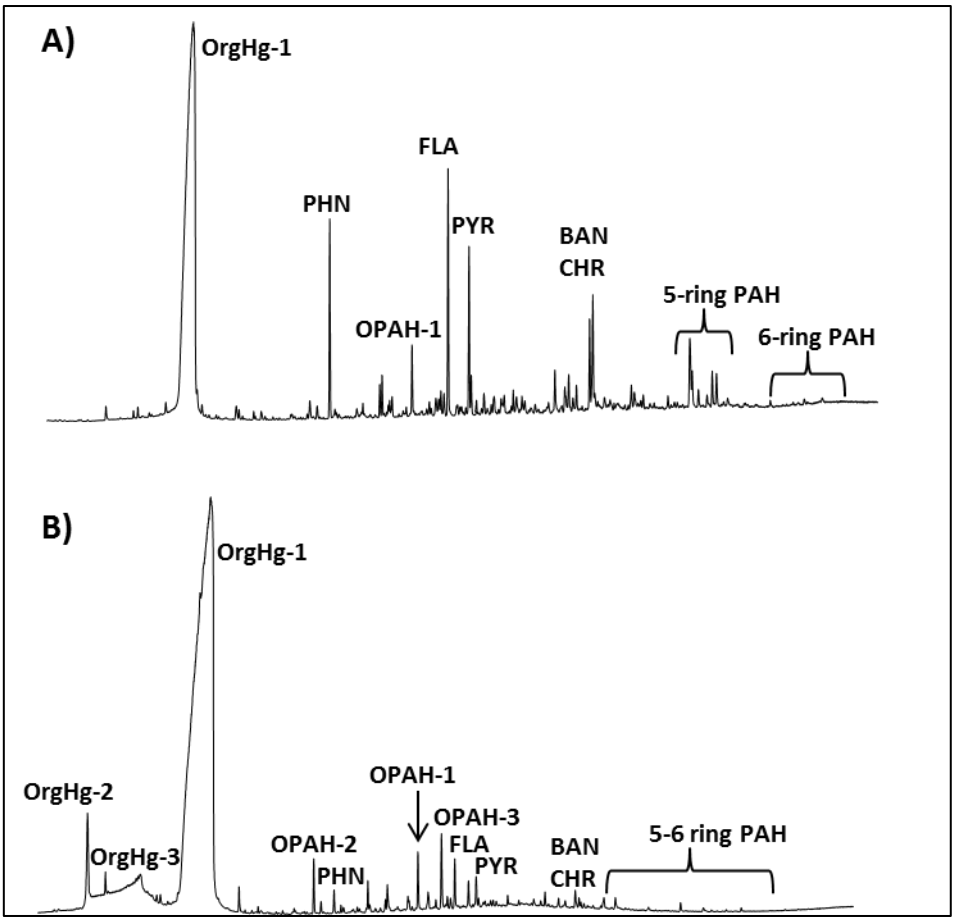

Figure 5: A) TIC chromatographic fingerprint of soot-stupp. B) TIC chromatographic fingerprint of flue dust. Note that elemental Hg (monitored using m/z 200 and 202) is present throughout part of the GC run (plateau).(OrgHg-1: Phenylmercury propionate; OrgHg-2: Benzyl(chloro)mercury; OrgHg-3: Mercury (II) chloride; OPAH-1 Anthraquinone; OPAH-2: Fluorenone; OPAH-3: 1,8 Naphthalic anhydride; PHN: phenanthrene; FLA: fluoranthene; PYR: pyrene; BAN: benz[a]anthracene; CHR: chrysene).

446 *3.4.4 Dioxins and furans*

447 The analyses (Table 3) showed that the polychlorinated dibenzo-p-dioxins (PCDDs)
448 were more abundant in mining waste than polychlorinated dibenzofurans (PCDFs).
449 Following the sink/source classification (Dömtörová et al., 2012; Wagrowski and Hites,
450 2000), this profile (PCDDs > PCDFs) is classified as ‘‘sink’’, for which PCDDs are
451 predominant (a ‘‘source’’ profile is characterized by a PCDF predominance). In
452 contrast, the opposite results were found for metallurgical waste (PCDFs > PCDDs),
453 thereby strongly suggesting that dioxins and furans were produced in the
454 pyrometallurgical process (see discussion).

455 Table 3: PCDF/PCDD congener profiles in the mining and metallurgical waste studied.
456 (F4 = 2378-TCDF, F5 = 12378-PeCDF + 23478-PeCDF; F6 = 123478-
457 HxCDF + 123678-HxCDF + 234678-HxCDF + 123789-HxCDF; F7 = 1234678-
458 HpCDF + 1234789-HpCDF; F8 = OCDF; D4 = 2378-TCDD; D5 = 12378-PeCDD;
459 D6 = 123478-HxCDD + 123678-HxCDD + 123789-HxCDD; D7 = 1234678-HpCDD;
460 D8 = OCDD.)

PCDF Congeners	pg/g			
	Spoil heap 1	**Spoil heap 2**	**Soot –Stupp**	**Flue dust**
F4	*1.2502*	*5.6955*	*37.3716*	*129.841*
F5	*0.6053*	*2.8659*	*22.7721*	*43.7394*
F6	*0.8046*	*3.5850*	*13.1185*	*13.3853*
F7	*1.2713*	*4.5573*	*4.2133*	*7.0533*
F8	*1.0610*	*3.0515*	*2.0404*	*6.1498*
Total	*4.9924*	*19.7552*	*79.5159*	*200.1688*

461

PCDD Congeners	pg/g			
	Spoil heap 1	**Spoil heap 2**	**Soot –Stupp**	**Flue dust**
D4	*0.0228*	*0.0632*	*0.0826*	*0.2339*
D5	*0.0522*	*0.1817*	*0.1257*	*0.3083*
D6	*2.1726*	*0*	*0*	*0*
D7	*1.7764*	*4.7866*	*7.6867*	*6.1844*
D8	*6.4191*	*15.6661*	*19.0688*	*11.5689*
Total	*10.4431*	*20.6976*	*26.9638*	*18.2955*

462

463

464

4. Discussion

The closure of Hg and As facilities in the 1970s was driven worldwide by international health concerns over their use. The abandonment of activity and continuous remobilization of the pollutants in the remaining waste piles make these sites significant environmental hazards (Gray et al., 2002; Millán et al., 2006; Navarro et al., 2009; Rieuwerts et al., 2014). In this context, when the mine and Hg-processing plant were operational at La Soterraña, heterogeneous waste materials in size and nature were disposed of in an unsystematic manner. In addition, the ulterior long-term abandonment of the area and the partial demolition of the buildings have led to an uncontrolled and uneven distribution of supplementary waste. Mining and metallurgical waste made up predominantly of relatively small remnants, as shown in this work (Fig 3.), have exposed an enormous surface area of sulphide/oxide minerals susceptible to reaction with water and/or air. Also, the emissions of polluting steam and particles and the dumping of waste have considerably affected the surrounding areas as a result of mechanical dispersion (wind erosion) of the spoil heaps, together with the abovementioned oxidation and lixiviation (Sierra et al., 2011). On the whole, the effect of the contamination on the environmental compartments is severe (Loredo et al., 2006; Matanzas et al., 2017) and risks associated with these former Hg-mining areas are of concern (Ordóñez et al., 2011). Of note, a recent study of a nearby site with similar characteristics estimated the release of 7 tons of As per year into a river (González-Fernández et al., 2018). Pollutant mobilization gains a further dimension as the spoil heaps are currently covered by incipient soil, which in turn is colonized by pioneer plants and used as pasture for cattle (Matanzas et al., 2017). Furthermore, the relevance of pollutant dispersal on La Soterraña site and other brownfields in the same area has been recently highlighted by studies of geological records located more than 50 km away from the site (Gallego et al., 2019; García-Ordiales et al., 2018). These "long-distance" effects can be clearly understood when considered the total mass of Hg and especially of As still present in the different waste (Table S1).

Our findings corroborate the high toxicity of Hg-mining and metallurgical waste (Gallego et al., 2015 and references therein). In this regard, As emerges as the most concerning pollutant because the abovementioned volumes and given that it shows a greater leachability potential, irrespective of the conditions of the tests (Table 1). Consequently, mobility/leachability have recently been the main focus of

498 nanoremediation and adsorption approaches to mitigate the impact of the types of waste
499 studied here (Ayala and Fernandez, 2019; Gil-Díaz et al, 2019) and in other industrial
500 areas (López et al., 2015).

501 In addition, our results also indicate that consideration should be given to the capacity
502 of C&D waste to contaminate. In this regard, although the average values of C&D
503 waste leachability appeared to be low (Table 2), the extremely high total content of Hg
504 and especially As in this material makes it hazardous. This reflection implies that future
505 site remediation programs must specifically address the treatment of C&D waste. In
506 fact, several studies have reported this type of waste to be a potential source of pollution
507 (Gao et al., 2015; Pecorini et al., 2017; Roussat et al., 2008; Townsend et al., 2004).
508 Indeed, it can be considered a potential repository of hazardous pollutants (Saca et al.,
509 2017), even in highly problematic areas, such as those affected by radioactive waste
510 (Diedenhofen et al., 2006). Several authors have also demonstrated non-negligible
511 release of contaminants from clean and mixed C&D waste on contaminated sites
512 (Butera et al., 2014). In this regard, the adsorption of Hg in several construction
513 materials has been described (Gao et al., 2014). In concordance with our work, Prieto-
514 Taboada et al., 2013 also demonstrated how buildings in an industrial port of dense
515 traffic were "supplied" with both inorganic and organic contaminants. Contrary to other
516 studies (Jang and Townsend, 2001), the presence of organic contaminants in our C&D
517 waste samples was not significant. However, the abundance of PAHs in metallurgical
518 waste stock-piled in the vicinity of the ruined buildings and the presence of fuel spills,
519 and probably of underground storage tanks still not located, suggest that future
520 remediation work should also consider organic compounds in C&D waste.

521 The speciation studies revealed that Hg and As persisted in the environment, mainly in
522 the form of their less toxic chemical species. On first inspection, inorganic Hg appeared
523 to predominate in the samples (Table 1). However, analysis of organic pollutants (see
524 below) revealed unexpected results that disprove this notion. In turn, As (III) had a
525 notable presence in the metallurgical waste. Indeed, a specific study of the nature of this
526 compound (Lara-Gonzalo et al., 2019) confirmed the presence of the oxide arsenolite as
527 the mineral containing As (III), as suggested in previous findings (Gallego et al., 2015;
528 Haffert and Craw, 2009). Our results also revealed that the most problematic residues
529 (metallurgical waste) are found in the fine-grain fraction, in coherence with their former
530 recovery in sedimentation chambers used in the pyrometallurgical process. In fact, for

these residues, d_{10} can even exceed 50% (Fig. 2), thereby increasing the likelihood of suspension-deposition and indicating that dust dispersal at the site is a critical issue from a toxicological perspective.

Regarding organic pollutants, the highest PAH concentrations were found in flue dust, i.e. the waste produced at the end of the metallurgical process, inasmuch they were carried with the residual gases through the ducts and chimneys and were condensed sequentially as the temperature decreased. In addition, stupp/soot waste also carried significant concentrations of PAHs (Table 2), as the fuel used (fuel oil and coal) in the old kilns was often in physical contact with the mineral during the roasting process. The abovementioned oxide arsenolite (Haffert and Craw, 2009) was the main by-product of this process, whereas Hg was mostly recovered in the condensation systems (Gallego et al., 2015). Nevertheless, organometallic compounds and an unburnt residue of the natural organic matter in the ores were also produced during the process and, consequently, the resulting waste contains both inorganic and organic components. Indeed, the GC-MS approach revealed key molecular features of the foreseen organic pollutant inputs. Several areas where fuel and PCB release/spills had occurred were identified. In addition, partially biodegraded fuel oil and mainly pyrogenic combustion-derived parent PAHs imprinted their signatures in the GC-MS data. Although the spilled fuel was found in a specific area, it was clearly evidenced (absence of alkyl-PAHs, PAHs distribution in Fig. S3, etc.) that the main source of PAHs in the area was pyrogenic. In this regard, the predominance of the pyrogenic component was verified in a complementary way by PAH ratios (Boehm, 2006; Yunker et al., 2002), such as Anthracene/Anthracene + Phenanthrene (0.09 ± 0.03 averaged in the mining and metallurgical waste) and Fluoranthene/Fluoranthene + Pyrene (0.61 ± 0.05), both indicating that PAHs originated from combustion (pyrogenic source). Together with PAHs, the abundance of Oxy-PAHs in the fingerprint of the chromatograms of the metallurgical waste was also noteworthy (Fig. 5). These compounds may be as abundant, persistent and toxic in the environment as their parent PAHs, and they are usually linked to weathering (biodegradation mainly) processes wherever PAHs are abundant (Idowu et al., 2019).

Studies addressing the presence of Hg-organometallic compounds (Fernández-Martínez et al., 2014; Rumayor et al., 2017) pointed to the link between Hg and organic matter. Specifically, Hg speciation obtained by thermal desorption of samples of the

564 metallurgical waste studied here revealed the abundance of Hg associated with organic
565 matter, also "Hg-rich" pyrite (Hg-FeS_2), Hg^0 and $HgCl_2$ (Rumayor et al., 2017). These
566 results are coherent with the presence of volatile Hg species (Hg^0, $HgCl_2$) in the GC-MS
567 study (see Fig. 5). However, our GC-MS data also highlighted the presence of
568 organometallic compounds (other than methyl- or ethyl-Hg), namely phenylmercury
569 propionate ($C_9H_{10}HgO_2$) (previously described in Gallego et al., 2015) and
570 benzyl(chloro)mercury (C_7H_7ClHg), and their notable abundance, especially in the flue
571 dust (Fig. 5). These highly toxic compounds (ECHA, 2011) may have been formed
572 through the combination of Hg and aromatic hydrocarbons during the cooling of the
573 gas/vapours flowing through the condensing system.

574 The abundance of pyrogenic PAHs in the metallurgical waste and the presence of
575 chloride in several molecules found on the site (PCBs, $HgCl_2$) further supported our
576 interest in studying the presence of dioxins (PCDD) and furans (PCDF). In fact, other
577 metallurgical processes have been identified as habitual sources of dioxins (Weber et
578 al., 2008). Our results (Table 3) revealed a significant concentration of PCDD and
579 especially PCDF in the metallurgical waste; i.e. the products that passed through the
580 former ducts and chimneys are a notable source of these extremely toxic compounds. In
581 this regard, it should be pointed out that our data (Table 3) imply that the toxic
582 equivalents (WHO PCDD/F-TEQ) for flue dust are 29.032 pg I-TEQ/g. This TEQ value
583 is not only significantly higher than those obtained recently in soil samples from a
584 heavily polluted brownfield located 20 km north of La Soterraña but also greater than
585 the regional backgrounds (values both below 20 pg I-TEQ/g, see Lara-Gonzalo et al.,
586 2015). A comparison of our findings with the concentrations of PCDD and PCDF
587 reported in other industrial/polluted areas (Dömötörová et al. 2012, Rada et al. 2015)
588 strongly suggest a notable contaminant load in La Soterraña. In the light of these and
589 other lines of evidence (source profile as indicated in section 3.4.4, levels markedly
590 above the background, etc.), we conclude that PCDD and PCDF in this brownfield were
591 generated during the pyrometallurgy of Hg-ores.

592

593

594

5. Conclusions

The brownfield of La Soterraña is a paradigmatic example of the combined effect of the abandonment (> 45 years) of mining/industrial facilities, inappropriate waste disposal, and the presence of highly toxic contaminants. Using a multifaceted, environmental forensics study carried out by means of a combination of advanced analytics, cartographic techniques and a historical study, we have identified features commonly overlooked by conventional analyses. The methodology described is likely to find application in other complex brownfields worldwide.

Here we focused on the wide range of waste that had been disposed of at La Soterraña over decades. These waste materials are subjected to weathering and thus are the main source of pollution on the site. Our results indicate that a notable volume of C&D waste should be considered hazardous, although metallurgical waste (the highest contents of Hg and As) and mining waste (the highest volume) are of maximum concern. The site revealed a complex speciation of As and Hg, and the presence of unexpected Hg-aromatic compounds (addressed by GC-MS molecular techniques).

The acquisition of complementary information from various analyses also revealed the occurrence of PAHs, oxy-PAHs and PCBs, together with the inorganic and organic compounds abovementioned. In this context, this study is the first to identify PCDD and PCDF as by-products of the Hg-metallurgical process. The accumulation of organic and organometallic pollutants strongly suggests that the study site poses an extreme environmental risk, even irrespective of its high concentration of inorganic As and Hg.

We consider that once the most hazardous waste has been removed from the site, the effectiveness of remediation strategies will be complicated by the presence of multiple pollutants and their synergistic and antagonistic interactions. In this context, the identification of target analytes through the forensics approach followed here will now facilitate future remediation measures.

Acknowledgments

This research was partially funded by the LIFE project UE-17-SUBPRODUCTS-LIFE16-481, and the project SV-17-HUNOSA-1 (University of Oviedo and HUNOSA). We would like also to thank the Environmental Assay Unit of the Scientific and Technical Services of the University of Oviedo for its technical support.

References

Ahn, J.S., Park, Y.S., Kim, J.Y., Kim, K.W. 2005. Mineralogical and geochemical characterization of arsenic in an abandoned mine tailings of Korea Environ Geochem Health, 27,147–157. https://doi.org/ 10.1007/s10653-005-0121-8.

Alker S., Joy V., Roberts P., Smith N., 2000. The Definition of Brownfield. J. Environ. Plann. Man.; 43: 49-69. https://doi.org/10.1080/09640560010766.

Álvarez-Ayuso, E., Otones, V., Murciego, A., García-Sánchez, A., Regina, I.S. 2012. Antimony, arsenic and lead distribution in soils and plants of an agricultural area impacted by former mining activities. Sci Total Environ., 439, 35-43. https://doi.org/10.1016/j.scitotenv.2012.09.023.

Ayala, J., Fernández, B. 2019. Industrial waste materials as adsorbents for the removal of As and other toxic elements from an abandoned mine spoil heap leachate: a case study in Asturias. J. Hazard. Mater., (in press). doi.org/10.1016/j.jhazmat.2019.121446.

Bindler R., Yu R., Hansson S., Classen N., Karlsson J. 2012. Mining, metallurgy and the Historical Origin of Mercury Pollution in Lakes and Watercourses in Central Sweden. Environ Sci Technol. 46, 7984-7991. https://doi.org/10.1021/es300789q.

Boehm, P.D. 2006. Polycyclic Aromatic Hydrocarbons (PAHs). In Murphy, B. L., Morrison, R.D (Eds.), Environmental Forensics: Contaminant Specific Guide, Academic Press, San Diego, CA. pp. 313-337.

Boente, C., Sierra, C., Martínez-Blanco, D., Menéndez-Aguado, J. M., Gallego, J. R. 2018. Nanoscale zero-valent iron-assisted soil washing for the removal of potentially toxic elements. J. Hazard. Mater., 350, 55-65. https://doi:10.1016/j.jhazmat.2018.02.016.

Butera, S., Christensen, T. H., Astrup, T. F. 2014. Composition and leaching of construction and demolition waste: Inorganic elements and organic compounds. J. Hazard. Mater., 276, 302-311. https://doi.org/10.1016/j.jhazmat.2014.05.033.

Chopin, E., Alloway, B.J., 2007. Trace element partitioning and soil particle characterization around mining and smelting areas at Tharsis, Ríotinto and Huelva, SW Spain. Sci. Total Environ. 373, 488–500. https://doi.org/10.1016/j.scitotenv.2006.11.037.

Diedenhofen, S., Wotruba, H., Weitkämper, L., Meier Kortwig, J. 2006. Development of a decontamination process for radioactively contaminated and activated concrete from dismantled nuclear power plants by activity separation. Paper presented at the IMPC 2006 - Proceedings of 23rd International Mineral Processing Congress, 2382-2387.

Dömötörová, M., Stachová Sejáková, Z., Kočan, A., Čonka, K., Chovancová, J., & FabiŠiková, A. 2012. PCDDs, PCDFs, dioxin-like PCBs and indicator PCBs in soil from five selected areas in Slovakia. Chemosphere, 89, 480-485. https://doi:10.1016/j.chemosphere.2012.05.106.

Douglas, G.S., Emsbo-Mattingly, S.D., Stout, S.A., Uhler, A.D., McCarthy, K.J., 2007. Chemical fingerprinting methods. In: Murphy, B. L., Morrison, R.D. (Eds.), Introduction to Environmental Forensics. Academic Press, New York, pp. 311-454.

ECHA (European Chemicals Agency), 2011. Background document to RAC and SEAC opinions on five phenylmercury compounds. Available at: http://echa.europa.eu/documents/10162/18c9392a-1f07-4eee-a358-e27ff9e2f172 (accessed November, 2019).

Evers, D.C., Keane, S.E., Basu, N., Buck, D., 2016. Evaluating the effectiveness of the Minamata Convention on Mercury: Principles and recommendations for next steps. Sci. Total Environ. 569-570, 888-903. https://doi.org/10.1016/j.scitotenv.2016.05.001.

Fernández, S., Poschenrieder, C., Marcenò, C., Gallego, J. R., Jiménez-Gámez, D., Bueno, A., Afif, E. 2017. Phytoremediation capability of native plant species living on Pb-Zn and Hg-As mining wastes in the cantabrian range, north of Spain. J. Geochem. Explor., 174, 10-20. https://doi.org/10.1016/j.gexplo.2016.05.015.

Fernández-Martínez, R., Loredo, J., Ordóñez, A., Rucandio I. 2014. Mercury availability by operationally defined fractionation in granulometric distributions of soils and mine wastes from an abandoned cinnabar mine. Environ. Sci.: Processes Impacts, 16, 1069-1075. https://doi.org/10.1039/C3EM00710C.

Gallego, J. R., Fernández, J. R., Díez-Sanz, F., Ordoñez, S., Sastre, H., González-Rojas, E., Peláez, A.I., Sánchez, J. 2007. Bioremediation for shoreline cleanup: In situ vs. on-site treatments. Environ. Eng. Sci., 24, 493-504. https://doi:10.1089/ees.2006.0091.

Gallego, J.R., Esquinas, N., Rodríguez-Valdés, E., Menéndez-Aguado, J.M., Sierra, C., 2015. Comprehensive waste characterization and organic pollution co-occurrence in a Hg and As mining and metallurgy brownfield. J. Hazard. Mater. 300, 561–571. https://doi.org/10.1016/j.jhazmat.2015.07.029.

Gallego, J. R., Rodríguez-Valdés, E., Esquinas, N., Fernández-Braña, A., Afif, E. 2016. Insights into a 20-ha multi-contaminated brownfield megasite: An environmental forensics approach. Sci. Total Environ., 563-564, 683-692. doi:10.1016/j.scitotenv.2015.09.153.

Gallego, J. L. R., Ortiz, J. E., Sánchez-Palencia, Y., Baragaño, D., Borrego, Á. G., Torres, T. 2019. A multivariate examination of the timing and accumulation of

potentially toxic elements at las conchas bog (NW Spain). Environ. Pollut., 254 https://doi.org/10.1016/j.envpol.2019.113048.

Gao, X., Gu, Y., Xie, T., Liu, Y., Huang, S., Zhao, Y. 2014. Simulation of gaseous mercury adsorption of different building materials. Tumu Jianzhu Yu Huanjing Gongcheng/Journal of Civil, Architectural and Environmental Engineering, 36, 112-118. https://doi.org/10.11835/j.issn.1674-4764.2014.06.019.

Gao, X., Gu, Y., Xie, T., Zhen, G., Huang, S., Zhao, Y. 2015. Characterization and environmental risk assessment of heavy metals in construction and demolition wastes from five sources (chemical, metallurgical and light industries, and residential and recycled aggregates). Environ. Sci. and Pollut. R., 22(12), 9332-9344. https://doi.org/10.1007/s11356-014-4058-2.

García-Ordiales, E., Covelli, S., Rico, J. M., Roqueñí, N., Fontolan, G., Flor-Blanco, G., Cienfuegos, P., Loredo, J. 2018. Occurrence and speciation of arsenic and mercury in estuarine sediments affected by mining activities (Asturias, northern Spain). Chemosphere, 198, 281-289. https://doi.org/10.1016/j.chemosphere.2018.01.146.

Gil-Díaz, M., Rodríguez-Valdés, E., Alonso, J., Baragaño, D., Gallego, J. R., Lobo, M. C. 2019. Nanoremediation and long-term monitoring of brownfield soil highly polluted with as and Hg. Sci. Total Environ, 675, 165-175. https://doi.org/10.1016/j.scitotenv.2019.04.183.

González-Fernández, B., Rodríguez-Valdés, E., Boente, C., Menéndez-Casares, E., Fernández-Braña, A., Gallego, J. R. 2018. Long-term ongoing impact of arsenic contamination on the environmental compartments of a former mining-metallurgy area. Sci. Total Environ, 610-611, 820-830. https://doi.org/10.1016/j.scitotenv.2017.08.135.

Gray J.E., Crock. J. G, Fey. D. L. 2002. Environmental geochemistry of abandoned mercury mines in West-Central Nevada. USA. Appl. Geochem. 17. 1069–1079. https://doi.org/10.1016/S0883-2927(02)00004-5.

Haffert, L., Craw, D., 2008. Mineralogical controls on environmental mobility of arsenic from historic mine processing residues. Appl. Geochem. 23, 1467–1483. https://doi.org/10.1016/j.apgeochem.2007.12.030.

Haffert, L., Craw D. 2009. Field quantification and characterization of extreme arsenic concentrations at a historic mine processing site, Waiuta, New Zealand. New Zeal. J. Geol. Geop., 52, 261-272. https://doi.org/10.1080/00288300909509890.

Hagmann, D. F., Kruge, M. A., Cheung, M., Mastalerz, M., Gallego, J. L. R., Singh, J. P, Krumins J.A., Li X.N., Goodey, N. M. 2019. Environmental forensic characterization of former rail yard soils located adjacent to the statue of liberty in the New York/New Jersey harbor. Sci. Total Environ, 690, 1019-1034. https://doi.org/10.1016/j.scitotenv.2019.06.495.

He, M., Tian, L., Braaten, H. F. V., Wu, Q., Luo, J., Cai, L.. Lin, Y. 2019. Mercury–Organic matter interactions in soils and sediments: Angel or devil? Bull. Environ. Contam. Toxicol., 102(5), 621-627. https://doi:10.1007/s00128-018-2523-1.

Higueras, P., Fernández-Martínez, R., Esbrí, J. M., Rucandio, I., Loredo, J., Ordóñez, A., Álvarez, R. 2015. Mercury soil pollution in spain: A review. In: Jiménez E., Cabañas B., Lefebvre G. (eds) Environment, Energy and Climate Change I. The Handbook of Environmental Chemistry, vol 32. Springer, Cham. https://doi.org/10.1007/698_2014_280.

Idowu, O., Semple, K. T., Ramadass, K., O'Connor, W., Hansbro, P., Thavamani, P. 2019. Beyond the obvious: Environmental health implications of polar polycyclic aromatic hydrocarbons. Environ. Int., 123, 543-557. https://doi.org/10.1016/j.envint.2018.12.051.

Jang, Y-C. Townsend, T. G. 2001. Occurrence of organic pollutants in recovered soil fines from construction and demolition waste. Waste Manag., 21(8), 703-715. https://doi.org/10.1016/S0956-053X(01)00007-1.

Kruge, M. A., Gallego, J. L. R., Lara-Gonzalo, A., Esquinas, N. 2018. Environmental forensics study of crude oil and petroleum product spills in coastal and oilfield settings: Combined insights from conventional GC-MS, thermodesorption-GC-MS, and pyrolysis-GC-MS. Oil spill environmental forensics case studies (pp. 131-155) https://doi.org/10.1016/B978-0-12-804434-6.00007-0.

Lara-Gonzalo, A., Kruge, M.A., Lores, I., Gutiérrez, B., Gallego, J.R., 2015. Pyrolysis GC–MS for the rapid environmental forensic screening of contaminated brownfield soil. Org. Geochem. 87, 9-20. https://doi.org/10.1016/j.orggeochem.2015.06.012.

Lara-Gonzalo, A., Kruge, M. A., Lara-Gómez, L. M., Gutiérrez-Iglesias, B., Gallego, J. R. 2019. Co-occurrence of organic and inorganic contaminants in former Hg-As mining sites. Abstract presented at the 29th International Meeting on Organic Geochemistry, IMOG 2019.

Liu G, Cai Y, O´ Driscoll N. 2012. Environmental Chemistry and Toxicology of Mercury. Wiley&Sons Inc., Hoboken, New Jersey.

López, F. A., Alguacil, F. J., Rodríguez, O., Sierra, M. J., Millán, R. 2015. Mercury leaching from hazardous industrial wastes stabilized by sulfur polymer encapsulation. Waste Manag., 35, 301-306. https://doi.org/10.1016/j.wasman.2014.10.009.

Loredo, J., Luque, C., García Iglesias, J. 1988. Conditions of formation of mercury deposits from the Cantabrian Zone (Spain). Bull. Mineral. 111, 393–400.

781 Loredo, J., Ordóñez, A., Gallego, J. R., Baldo, C., García-Iglesias, J. 1999.
782 Geochemical characterisation of mercury mining spoil heaps in the area of Mieres
783 (Asturias, Northern Spain). J. Geochem. Exp., 67(1-3), 377-390. doi:10.1016/S0375-
784 6742(99)00066-7.

785 Loredo, J., Ordóñez, A., Álvarez, R. 2006. Environmental impact of toxic metals and
786 metalloids from the muñón cimero mercury-mining area (Asturias, Spain). J. Hazard.
787 Mater, 136(3), 455-467. https://doi.org/10.1016/j.jhazmat.2006.01.048.

788 Luque, C. 1985. Las mineralizaciones de mercurio de la Cordillera Cantábrica.
789 Unpublished doctoral thesis, University of Oviedo.

790 Matanzas, N., Sierra, M. J., Afif, E., Díaz, T. E., Gallego, J. R., Millán, R. 2017.
791 Geochemical study of a mining-metallurgy site polluted with as and hg and the transfer
792 of these contaminants to equisetum sp. J. Geochem. Explor. 182, 1-9.
793 https://doi.org/10.1016/j.gexplo.2017.08.008.

794 Millán, R., Gamarra, R., Schmid, T., Sierra, M. J., Quejido, A. J., Sánchez D. M.,
795 Cardona AI, Fernández M, Vera, R. 2006. Mercury content in vegetation and soils of
796 the Almadén mining area (Spain). Sci. Total Environ, 368, 79-87.
797 https://doi.org/10.1016/j.scitotenv.2005.09.096.
798
799 Moore, J.N., Luoma, S.N. 1990. Hazardous wastes from large-scale metal extraction. A
800 case study. Environ. Sci. and Technol. 24, 1278-1285.

801 Morrison, R.D., Murphy, B.L. 2006. Environmental forensics, Contaminant Specific
802 Guide. Academic Press.

803 Navarro, A., Cardellach, E., Corbella, M. 2009. Mercury mobility in mine waste from
804 Hg-mining areas in Almería, Andalusia (SE Spain). J. Geochem. Explor, 101, 236-246.
805 https://doi.org/10.1016/j.gexplo.2008.08.004.

806 Nikonova A. A., Gorshkov A. 2011. Rapid Chromatography for the Determination of
807 Polychlorinated Biphenyls by GC-MS in Environmental Monitoring. Anal. Lett 44,
808 1290-1300. https://doi.org/10.1080/00032719.2010.546024.
809
810 Ordóñez, A., Alvarez, R., Charlesworth, S., De Miguel, E., Loredo, J. 2011 Risk
811 assessment of soils contaminated by mercury mining, Northern Spain. J. Environ.
812 Monit., 13, 128-136, https://doi.org/10.1039/c0em00132e.

813 Pecorini, I., Baldi, F., Bacchi, D., Carnevale, E. A., Corti, A. 2017. Leaching behaviour
814 of hazardous waste under the impact of different ambient conditions. Waste Manag., 63,
815 96-106. https://doi.org/10.1016/j.wasman.2016.10.037.

816 Prieto-Taboada N, Ibarrondo I, Gómez-Laserna O, Martinez-Arkarazo I, Olazabal M.A,
817 Madariaga J.M. 2013. Buildings as repositories of hazardous pollutants of

818 anthropogenic origin. J Hazard Mater 248–249:451–460.
819 https://doi.org/10.1016/j.jhazmat.2013.01.008.

820 Rada, E. C., Ragazzi, M., Marconi, M., Chistè, A., Schiavon, M., Fedrizzi, S., Tava, M.
821 2015. PCDD/Fs in the soils in the province of Trento: 10 years of monitoring. Environ
822 Monit Assess. 187, 1-12. http://doi:10.1007/s10661-014-4114-x.

823 Rieuwerts, J.S. Mighanetara K.,. Braungardt , C.B, Rollinson, G.K. Pirrie D, Azizi. F.
824 2014. Geochemistry and mineralogy of arsenic in mine wastes and stream sediments in
825 a historic metal mining area in the UK. Sci. Total Environ 472, 226–234.
826 https://doi.org/10.1016/j.scitotenv.2013.11.029.

827 Roussat, N., Méhu, J., Abdelghafour, M., Brula, P. 2008. Leaching behaviour of
828 hazardous demolition waste. Waste Manag. 28, 2032-2040.
829 https://doi.org/10.1016/j.wasman.2007.10.019.

830 Rumayor, M., Gallego, J. R., Rodríguez-Valdés, E., Díaz-Somoano, M. 2017. An
831 assessment of the environmental fate of mercury species in highly polluted brownfields
832 by means of thermal desorption. J. Hazard. Mater., 325, 1-7.
833 https://doi.org/10.1016/j.jhazmat.2016.11.068.
834
835 Saca, N., Dimache, A., Radu, L. R., Iancu, I. 2017. Leaching behavior of some
836 demolition wastes. J Mater Cycles Waste Manag, 19, 623-630.
837 https://doi.org/10.1007/s10163-015-0459-7.

838 Sierra, C., Menéndez-Aguado, J.M., Afif, E., Carrero, M., Gallego, J.R., 2011.
839 Feasibility study on the use of soil washing to remediate the As–Hg contamination at an
840 ancient mining and metallurgy area. J. Hazard. Mater. 196, 93–100.
841 https://doi.org/1010.1016/j.jhazmat.2011.08.080.
842
843 Sierra, C., Álvarez Saiz, J. R., Gallego, J. L. R. 2013. Nanofiltration of acid mine
844 drainage in an abandoned mercury mining area. Water Air Soil Pollut, 224: 1734.
845 https://doi.org/10.1007/s11270-013-1734-7.
846
847 Somasundaram, S., Jeon, T-W, Kang, Y-Y., Kim, W-I., Jeong, S-K., Kim, Y-J., Jeong
848 J-M., Shin, S. K. 2015. Characterization of wastes from construction and demolition
849 sector. Environ Monit Assess, 187, 4200. https://doi.org/10.1007/s10661-014-4200-0.

850 Staunton, J. A., Mc Donnell, R. J., Gormally, M. J., Williams, C. D., Henry, T.,
851 Morrison, L. 2014. Assessing metal contamination from construction and demolition
852 (C&D) waste used to infill wetlands: Using *deroceras reticulatum* (mollusca:
853 Gastropoda). Environ Sci Process Impacts, 16 (11), 2477-2487.
854 https://doi.org/10.1039/c4em00300d.

855 Tarvainen, T., Albanese, S., Birke, M., Poňaviĉ, M., Reimann, C., The GEMAS Project
856 Team. 2013. Arsenic in agricultural and grazing land soils of Europe. Appl. Geochem.,
857 28, 2-10. https://doi.org/10.1016/j.apgeochem.2012.10.005.

Thavamani P., Megharaj M., Krishnamurti G.S., McFarland R, Naidu R. 2011. Finger printing of mixed contaminants from former manufactured gas plant (MGP) site soils: implications to bioremediation. Environ. Int. 37, 184–189. https://doi.org/10.1016/j.envint.2010.08.017.

Townsend T., Tolaymat T., Leo K., Jambeck J. 2004. Heavy metals in recovered fines from construction and demolition debris recycling facilities in Florida. Sci Total Environ 332, 1–11. https://doi.org/10.1016/j.scitotenv.2004.03.011.

Uhler, A.D., Stout, S.A., Emsbo-Mattingly, S.D., Rouhani, S. 2010. Chemical fingerprinting: streamlining site assessment during the sustainable redevelopment process. In: Brown, K., et al. (Eds.), Sustainable Land Development and Restoration: Decision Consequence Analysis. Elsevier Butterworth-Heinemann, NewYork, pp. 311–323.

UNEP, 2013. Global Mercury Assessment 2013: Sources, Emissions, Releases and Environmental Transport. UNEP Chemicals Branch, Geneva, Switzerland.

Wagrowski, D.M., Hites, R.A. 2000. Insights into the global distribution of polychlorinated dibenzo-p-dioxins and dibenzofurans. Env. Sci. Tech., 34, 2952-2958. https://doi:10.1021/es991138o.

Wang, S., Mulligan, C.N. 2006. Occurrence of Arsenic Contamination in Canada: Sources, Behavior and Distribution. Sci. Total Environ, 366, 701-721. https://doi.org/10.1016/j.scitotenv.2005.09.005.

Wang, Z., Guo, H., Xiu, W., Wang, J., Shen, M., 2018. High arsenic groundwater in the Guide basin, northwestern China: Distribution and genesis mechanisms. Sci. Total Environ. 640–641, 194–206. https://doi.org/10.1016/j.scitotenv.2018.05.255.

Weber R., Gaus C., Tysklind M., Johnston .P, Forter M., Hollert H., Heinisch E., Holoubek I., Lloyd-Smith M., Masunaga S., Moccarelli P., Santillo D., Seike N., Symons R., Torres J.P., Verta M., Varbelow G., Vijgen J., Watson A., Costner P.,

Woelz J., Wycisk P., Zennegg M. 2008 Dioxin and POP-contaminated sites – contemporary and future relevance and challenges. Environ Sci Pollut Res Int. 15, 363-393. https://doi.org/10.1007/s11356-008-0024-1.

Wilkin, R.T., Lee, T.R., Beak, D.G., Anderson, R., Burns, B., 2018. Groundwater co-contaminant behavior of arsenic and selenium at a lead and zinc smelting facility. Appl. Geochem. 89, 255–264. https://doi.org/10.1016/j.apgeochem.2017.12.011.

Yunker, M.B., Macdonald, R.W., Vingarzan, R., Mitchell, R.H., Goyette, D., Sylvestre, S. 2002. PAHs in the Fraser River basin: A critical appraisal of PAH ratios as indicators of PAH source and composition. Org. Geochem. 33, 489–515. https://doi.org/10.1016/S0146-6380(02)00002-5.

Supplementary material for on-line publication only

Click here to download Supplementary material for on-line publication only: Fernandez et al 2020 STOTEN supplementary mater

***conflict of Interest Statement**

Declaration of interests

☒ The authors declare that they have no known competing financial interests or personal relationships that could have appeared to influence the work reported in this paper.

☐The authors declare the following financial interests/personal relationships which may be considered as potential competing interests: